



Mersin Photogrammetry Journal

<https://dergipark.org.tr/en/pub/mephoj>

e-ISSN 2687-654X



3D modeling of car parts by photogrammetric methods: Example of brake discs

Engin Kanun ^{*1}, Ganime Melike Oğuz ², Murat Yakar ³

¹Mersin University, Faculty of Engineering, Department of Mechanical Engineering, Mersin, Türkiye

²ESC Engineering, Geomatics Engineer, Adana, Türkiye

³Mersin University, Faculty of Engineering, Department of Geomatics Engineering, Mersin, Türkiye

Keywords

Reverse Engineering
3D modeling
Photogrammetry
Brake discs

Research/Review Article

DOI:10.53093/mephoj.1131619

Received:16.06.2022

Accepted:04.07.2022

Abstract

Re-measurement of existing, manufactured parts and re-creation of 3D models of these parts brought about the concept of reverse engineering. Reverse engineering has become a frequently applied and utilized concept in processes such as repairing damaged parts, improving used parts, and making new designs based on old parts. One of the main reverse engineering methods widely used by many engineering branches is photogrammetry. Photogrammetry, which includes a wide range of applications from professional cameras to mobile phones, is divided into branches such as terrestrial photogrammetry, aerial photogrammetry and underwater photogrammetry. The basis of all these categories is the concept of making measurements of a part, structure or region and modeling them in 3D, even if they involve different equipment and instruments. In this study, the 3D model of a rear brake disc of a personal passenger car was obtained using mobile photogrammetric methods. In the results section, the applicability of the method was examined in terms of cost, time and accuracy, together with the results of the accuracy analysis. It has been shown that the mobile photogrammetry method can provide easy applicability, low cost and high accuracy of 0.88 mm.

1. Introduction

The popularity of reverse engineering applications is increasing progressively. Not only engineers, but also many professions such as architects, archaeologists, biologists, medics and historians use these applications which are becoming more and more comprehensive and developing [1-7].

Some of the examples of reverse engineering applications of mechanical engineering are 3D modeling and prototyping of a damaged helical gear [8], 3D modeling and simulation of milling tools [9], 3D model generation of a plate and determination of heat transfer properties [10], 3D modeling and deformation analysis of roof bolts [11], simulating the resistance spot welding process of a panel and deformation analysis [12], 3D modeling of antique machines and transferring them to future generations [13] and 3D modeling and flow analysis of a damaged turbocharger [14].

The aviation industry is another branch that utilizes reverse engineering methods. For instance: 3D modeling of micro-grooved wings and investigation of their flow characteristics [15], assembly inspection of large aircrafts with non-contact measurements [16], investigation of airframes and aerodynamic surfaces using LiDAR sensors [17].

Another branch in which reverse engineering applications are used is the maritime sector. There are many reverse engineering applications utilized in shipyards, marinas, offshore platforms, and ships under cruising. Ship hull shape modelling, hull shape measurements and corrections, damage analysis and repairs with the application of photogrammetry based systems [18], 3D modeling of the main drive propeller shaft housing and detection of manufacturing defects [19], hull form and propeller modeling and their comparison with project data [20-22], 3D modeling of submarines [23], production of a prototype of a fishing boat using photogrammetric and terrestrial laser

* Corresponding Author

(ekanun@mersin.edu.tr) ORCID ID 0000-0002-2369-5322
(melikoguzz@gmail.com) ORCID ID 0000-0003-0241-6870
(myakar@mersin.edu.tr) ORCID ID 0000-0002-2664-6251

Cite this article

Kanun, E., Oğuz, G. M., & Yakar, M. (2022). 3D modeling of car parts by photogrammetric methods: Example of brake discs. *Mersin Photogrammetry Journal*, 4(1), 07-13

scanning methods [24], 3D modeling of underwater remains of historic ships [25], overall efficiency assessment and hydrodynamic performance calculations of a trawler propulsion system [26] can be given as examples of the concept of using reverse engineering applications in the maritime industry.

There are many reverse engineering applications for the documentation of cultural heritage. Geomatics engineers, city planners, historians, archaeologists and anthropologists take part in the documentation of cultural heritage and carry out scientific studies. In all these processes, it is necessary to avoid damaging the objects while performing the measurements and 3D modeling of the artifacts. For this reason, reverse engineering studies are carried out with advanced methods such as terrestrial photogrammetry, aerial photogrammetry, underwater photogrammetry, mobile photogrammetry, terrestrial laser scanning, underwater laser scanning, and aerial laser scanning. 3D modeling of a historic castle [27], documentation of historical caravansaries by digital close range photogrammetry [28], 3D modeling of a mausoleum using a terrestrial laser scanner [29] are some examples of documenting cultural heritage using reverse engineering methods.

In this study, close range photogrammetry, which is one of the reverse engineering methods mentioned above, was used. Close range photogrammetry includes a calibrated camera, marked points on the object, and computer as shown in the “Fig. 1”.

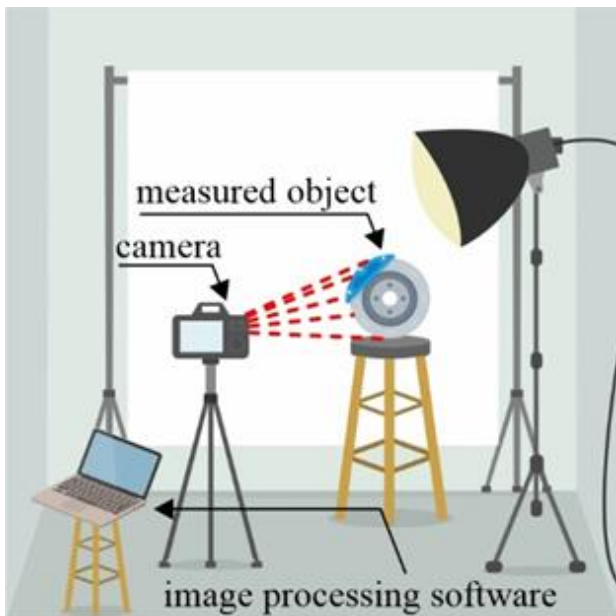


Figure 1. Photogrammetric measurement components

Marked points are pasted on the object to be measured. The camera takes several photos of objects from different directions to create two-dimensional digital images. Using picture recognition technology, the location of marked points can be determined in the computer [30]. The coordinates of marked points, as well as the camera's position and orientation, can be calculated using the correlation equation and mathematical model [31].

High measuring accuracy is one of the most essential characteristics of close-range photogrammetry. In the

case of a high configuration, relative accuracy in the single-camera measuring system can reach $5\mu\text{m} + 5\mu\text{m}/\text{m}$. High efficiency is another characteristic of close-range photogrammetry. Obtaining data on tens of thousands of data points in a short period of time is possible using this method. Another remarkable feature of close-range photogrammetry is stable performance. Even in the presence of adverse conditions such as vibration, high temperature, high pressure, and hazardous locations, high accuracy readings can be achieved. Measuring without contact is another significant property of close-range photogrammetry, thus the object to be measured is not damaged at all [30].

One of the most important inventions of mankind, which has made many inventions from the past to the present, is undoubtedly the automobile. In this industry, which has been open to development and innovation throughout history, the safety systems of vehicles are also being improved day by day. When it comes to automobile safety systems, one of the first and most significant systems that comes to mind is brake systems. Currently, the most used braking system is the system consisting of disc (rotor), caliper, piston and pads as shown in the “Fig. 2”.

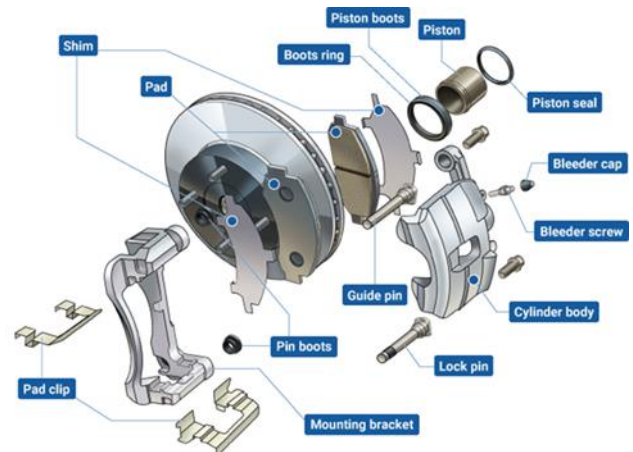


Figure 2. Components of disc brakes [32]

Disc brake rotors rotate with the wheels, and brake pads attached to the brake calipers clamp down on these rotors to stop or slow the wheels. Friction is created when the brake pads press against the rotors, converting kinetic energy to thermal energy. This thermal energy produces heat, but because the major components are exposed to the atmosphere, the heat is effectively diffused. This heat-dissipating feature helps to prevent brake fade, which is when the heat affects braking performance. Another benefit of disc brakes is its resistance to water fade, which happens when water on the brakes reduces braking force dramatically. The rotor rotates at high rates as the vehicle is moving, and this rotational motion discharges the water from the rotors, resulting in a consistent braking force [32].

The aim of this study is to investigate whether automobile parts can be modeled in 3D by mobile photogrammetry method, which is the process of creating a 3D model of an object by taking photos from different angles via a mobile phone. In this study, the right rear brake disc of the 2012 model Citroën C4 B7 has

been examined. First, the brake disc was disassembled from the vehicle. Photographs were taken to obtain the 3D model, and finally, the obtained model was examined. The pre-measurements on the brake disc and the dimensions of the created 3D CAD model were compared, accuracy analysis was made and presented in the results section.

As a result, the method used was examined in terms of accuracy, cost, time and applicability. Since the obtained 3D model can be used in various works such as maintenance-repair, restoration, prototyping, product development, and improvement of old designs, this study has the feature of being a guide for those who want to do this job in the market [33-35].

2. Method

In this paper, smartphone-based photogrammetric survey was implemented to obtain the 3D model of the right rear brake disc which is examined in this study. The brake disc was dismantled from a 2012 Citroën C4 B7 1.6 VTi car.



Figure 3. Brake disc removal step

Although the front brake discs of this vehicle are ventilated, the rear discs are solid. Solid brake discs, which have less design details than ventilated brake discs, are more suitable for modeling with photogrammetric methods. For this reason, modeling ventilation ducts and holes correctly in 3D would give low accuracy with the photogrammetric method.



Figure 4. Front and rear view of disassembled brake disc

This study consists of two phases such as field work and office work. During the field work, photogrammetric images were captured with the aim of obtaining the 3D model of the brake disc. At the stage of office work, the photos were uploaded to the computer for processing and a 3D model was obtained.

2.1. Specifications and Features of the Camera

Digital images of the brake disc were acquired by using Samsung Galaxy S10 mobile phone. The mobile phone has three rear cameras. The main camera of the phone has 12- megapixels with a 5.6x4.2 mm sensor size. Auto-focusing and focusing at infinity settings were applied. The minimum focusing distance of the camera is 0.10 m and the hyperfocal distance of the camera is 3.60 m. The lens of the camera has a focal length of 4.32 mm and (f/1.5) aperture. Focal length (35 mm eq.) is 27.7714 mm. In addition, the lens has a 66.3° horizontal field of view and 52.2° vertical field of view. Magnification factor was 1x for all photos taken. In addition to all these, camera calibration was performed and the calibration coefficients of the camera were calculated.



Figure 5. Smartphone used for data acquisition

2.2. Camera Calibration

One of the requirements for obtaining a highly accurate photogrammetric model is camera calibration. As a result of the camera calibration, the camera distortion parameters of the lens are calculated. Thus, depth maps are obtained more accurately and high precision is achieved.

For this reason, within the scope of the study, photographs of the chessboard seen in “Fig. 6” were taken from different angles and transferred to the computer. The photos taken were processed in the camera calibration module of Agisoft Metashape Professional software and the distortion parameters were calculated.

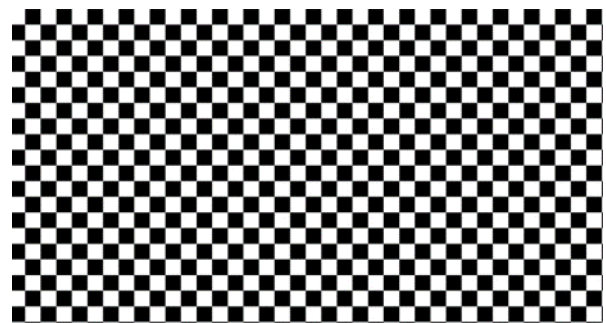


Figure 6. Chessboard used for camera calibration

The results of the camera calibration parameters obtained from calibration process shown at the “Table 1”:

Table 1. Camera calibration results

Parameter	Value	Parameter	Value
f	3095.89482	cx	-34.863
k1	0.346132	cy	-2.22197
k2	-2.4963	p1	0.000972003
k3	6.41376	p2	0.000524342
k4	-5.52763	b1	-0.899219
		b2	-1.56922

2.3. Data Acquisition

The front and rear faces of the brake disc were modeled separately and then assembled. For this reason, 191 photographs of the brake disc, which was disassembled from the car, were taken from different angles and from different distances as shown in “Fig. 7 and 8”. A portable spotlight was used to provide the right lighting during the photo shoots. Blurry photos, flash light, optical stabilization, digital zoom, and fish-eye lenses were avoided in order to produce better results.

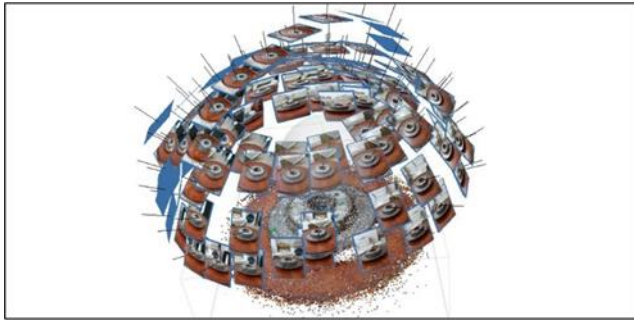


Figure 7. Camera stations configuration of brake disc (front)

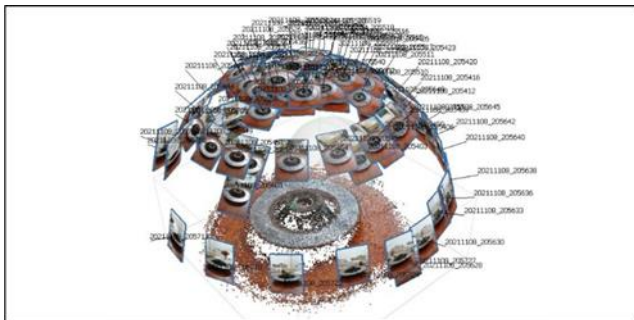


Figure 8. Camera stations configuration of brake disc (rear)

2.4. Data Processing

After the completion of the field work, the office work phase was initiated. During the office phase of the study, 191 of the images were processed at Agisoft Metashape Professional Software. Two user tie points were marked on every component of the brake disc to submit an accurate triangulation to the photos. Then, by taking precise measurements on the parts of the brake disc, predefined positioning and scale constrains were generated with two user tie points that marked before as seen in the “Fig. 9”. Generic block type option was selected with the aim of helping the triangulation process. Since the camera calibration parameters have

already been calculated, ‘Keep camera calibration’ option was selected for aerotriangulation process. The points (numbered 1 to 4), shown in yellow in Figure 9, are marked in all photographs so that the camera positions are accurately determined and the point cloud data is as noise-free as possible.



Figure 9. User tie points and scale constrains of the brake disc

After the aerotriangulation process, 3D point cloud data generation step was initiated. Colored point cloud was constructed by selecting the options of 1 pixels point sampling, no-compression, and visible colors for color source. On the obtained point cloud data, the points belonging to the unwanted regions were roughly cleaned. In this way, unnecessary processing power usage and time wastage were avoided during the process.

After cleaning the redundant points in the sparse point cloud data, dense point cloud data was generated applying moderate depth filtering. For the front side of the brake disc, sparse point cloud data contains 143,040 points, while dense point cloud data contains 1,266,657 points. As for the rear side, sparse point cloud data contains 83,821 points, while dense point cloud data contains 1,375,748 points. Sparse and dense point cloud data of the front and rear surfaces of the brake disc are shown in “Fig. 10 and 11”.



Figure 10. Sparse and dense point cloud data (front)



Figure 11. Sparse and dense point cloud data (rear)

During the mesh building process, source data was selected as dense cloud. Surface type was selected as arbitrary (3D) and high-quality face count was applied. Interpolation was enabled and calculate vertex colors option was marked. All these processes were applied separately for the front and rear surfaces of the brake disc, and the final version of the 3D brake disc model was obtained by combining the 2 models obtained at the end.

3. Results and Discussion

“Fig. 12” shows the 3D photogrammetric model of the brake disc. There are 467,929 total Triangulated Irregular Networks (TIN) grids on the model.

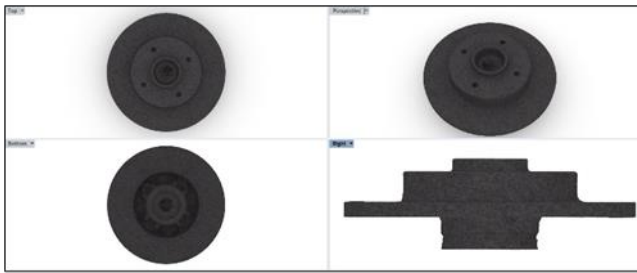


Figure 12. 3D solid model of the brake disc from different views

Considering the significance of design verification in the overall reverse engineering phase, few, if any, publications on part-to-CAD reverse engineering discuss modeling accuracy [36]. After obtaining the 3D photogrammetric model of the brake disc, accuracy analysis was performed on the model. The measurements taken on the brake disc before starting the photo acquisition were compared with the measurements of the 3D photogrammetric model obtained as a result of the study. “Fig. 13” presents the lengths compared on the object. The root mean square error values obtained are presented in “Table 2”:

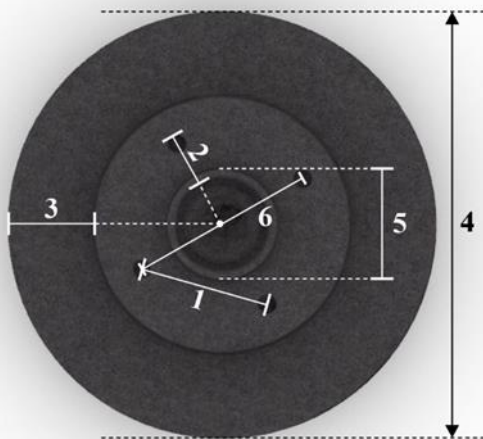


Figure 13. The lengths compared on the object

According to “Table 2”, the 3D model of the brake disc has a total root mean square error (RMSE) of **0.88 mm**.

In addition to the dimensional accuracy analysis, point deviation analysis was also performed. The deviation between the obtained point cloud data and the

surface of the solid model was analyzed separately for the front and rear faces of the brake disc. “Fig. 14” and “Fig. 15” present the results of the point deviation analysis of the front and rear surfaces of the brake disc. As can be seen in the figures, most of the points overlap with the solid model surface. Holes and sharp edges on the object are the parts where point deviations are most evident. According to the color scale, the blue colored dots exactly overlap with the surface, while the red colored dots are the places with relatively high deviations.

Table 2. Accuracy assessment results [in mm]

Length	Real	Model	V	VV
1	81	81.4	0.4	0.16
2	35	33.8	1.2	1.44
3	53	54.1	1.1	1.21
4	247	246.4	0.6	0.36
5	70	70.8	0.8	0.64
6	95	94.1	0.9	0.81

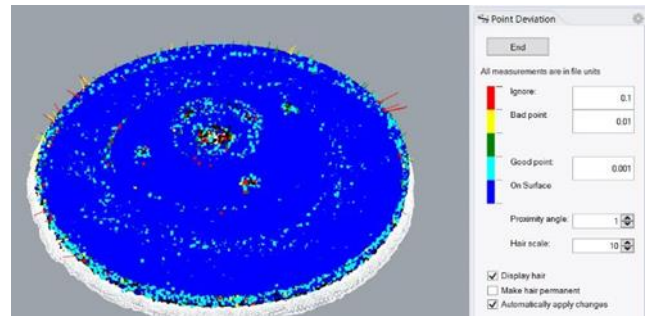


Figure 14. Point deviation analysis of the front side

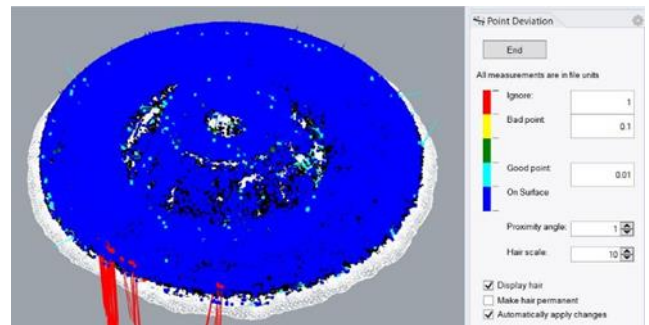


Figure 15. Point deviation analysis of the rear side

Keypoints density average, calculated by the software, is 5541 points per image. Reprojection error is 0.85 pixels. “Table 3” presents the position uncertainties of computed images.

Table 3. The position uncertainties of computed images

	X [units]	Y [units]	Z [units]
Minimum	0.0012	0.00106	0.00144
Mean	0.00352	0.00347	0.00384
Maximum	0.01309	0.01622	0.02073

4. Conclusion

To summarize, the concept of reverse engineering was mentioned in this study. Examples of the use of photogrammetry, which is one of the most frequently

used reverse engineering methods, in the literature are given. It has been shown that car parts can be modeled with high accuracy and in three dimensions by photogrammetric methods. In the next study, it is planned to model the same part with a handheld laser scanner. The results will be compared and it will be discussed which method is more suitable for modeling such parts. This study also has the feature of being a guide for those who will do this job in the market.

Acknowledgement

The authors would like to thank the members of Mersin University Department of Geomatics Engineering for their contribution to this study.

Author contributions

Engin Kanun: Data curation, Writing-Original draft preparation, Software, Validation. **Ganime Melike Oğuz:** Visualization, Investigation, Writing-Reviewing and Editing. **Murat Yakar:** Conceptualization, Methodology, Software.

Conflicts of interest

The authors declare no conflicts of interest

References

1. Yakar, M., Murat Yılmaz, H., Yıldız, F., Zeybek, M., Şentürk, H., & Çelik, H. (2009). Silifke-Mersin Bölgesinde Roma Dönemi Eserlerinin 3 Boyutlu Modelleme Çalışması ve Animasyonu. *Jeodezi ve Jeoinformasyon Dergisi*, (101).
2. Şanlıoğlu, İ., Zeybeka, M., & Karauğuzb, G. (2013). Photogrammetric survey and 3D modeling of İvrız rock relief in LATE Hittite Era. *Mediterranean Archaeology & Archaeometry*, 13(2).
3. Yakar, M., & Doğan, Y. (2018). GIS and three-dimensional modeling for cultural heritages. *International Journal of Engineering and Geosciences (IJEG)*, 3(2), 50-55.
4. Unal, M., Yakar, M., & Yildiz, F. (2004, July). Discontinuity surface roughness measurement techniques and the evaluation of digital photogrammetric method. In *Proceedings of the 20th international congress for photogrammetry and remote sensing, ISPRS* (Vol. 1103, p. 1108).
5. Yakar, M., Yılmaz, H. M., Güleç, S. A., & Korumaz, M. (2009). Advantage of digital close range photogrammetry in drawing of muqarnas in architecture. *Information Technology Journal*, 8(2), 202-207.
6. Alyilmaz, C., Yakar, M., & Yılmaz, H. M. (2010). Drawing of petroglyphs in Mongolia by close range photogrammetry. *Scientific Research and Essays*, 5(11), 1216-1222.
7. Yılmaz, H. M., Karabörk, H., & Yakar, M. (2000). Yersel fotogrametrinin kullanım alanları. *Niğde Üniversitesi Mühendislik Bilimleri Dergisi*, 4(1), 1.
8. Şahin, İ., Şahin, T., & Gökçe, H. (2017). Hasarlı Dişlilerin Tersine Mühendislik Yaklaşımıyla Yeniden Oluşturulması. *Düzce Üniversitesi Bilim ve Teknoloji Dergisi*, 5(2), 485-495.
9. Che, J., Zhang, Y., Wang, H., Liu, Y., Du, M., Ma, S., ... & Suo, C. (2021). A novel method for analyzing working performance of milling tools based on reverse engineering. *Journal of Petroleum Science and Engineering*, 197, 107987.
10. Zhang, L., Yuan, J., He, S., Huang, S., Xiong, S., Shi, T., & Xuan, J. (2021). Contact heat transfer analysis between mechanical surfaces based on reverse engineering and FEM. *Tribology International*, 161, 107097.
11. Singh, S. K., Raval, S., & Banerjee, B. (2021). A robust approach to identify roof bolts in 3D point cloud data captured from a mobile laser scanner. *International Journal of Mining Science and Technology*, 31(2), 303-312.
12. Liu, X., Wei, Y., Wu, H., & Zhang, T. (2020). Factor analysis of deformation in resistance spot welding of complex steel sheets based on reverse engineering technology and direct finite element analysis. *Journal of Manufacturing Processes*, 57, 72-90.
13. LaRocco, J., & Paeng, D. G. (2020). A functional analysis of two 3D-scanned antique pistols from New Zealand. *Virtual Archaeology Review*, 11(22), 85-94.
14. Kanun, E. (2021). Using photogrammetric modeling in reverse engineering applications: Damaged turbocharger example. *Mersin Photogrammetry Journal*, 3(1), 21-28.
15. Chitsaz, N., Siddiqui, K., Marian, R., & Chahl, J. (2021). An experimental study of the aerodynamics of micro corrugated wings at low Reynolds number. *Experimental Thermal and Fluid Science*, 121, 110286.
16. Liang, B., Liu, W., Liu, K., Zhou, M., Zhang, Y., & Jia, Z. (2021). A Portable Noncontact Profile Scanning System for Aircraft Assembly. *Engineering*.
17. Aldao, E., González-Jorge, H., & Pérez, J. A. (2021). Metrological comparison of LiDAR and photogrammetric systems for deformation monitoring of aerospace parts. *Measurement*, 174, 109037.
18. Koelman, H. J. (2010). Application of a photogrammetry-based system to measure and re-engineer ship hulls and ship parts: An industrial practices-based report. *Computer-Aided Design*, 42(8), 731-743.
19. Deja, M., Dobrzyński, M., & Rymkiewicz, M. (2019). Application of reverse engineering technology in part design for shipbuilding industry. *Polish Maritime Research*, 26(2), 126-133. <https://doi.org/10.2478/pomr-2019-0032>
20. Kanun, E., & Yakar, M. (2021). Mobile phone-based photogrammetry for 3D modeling of ship hulls. *Mersin University Journal of Maritime Faculty*, 3(1), 9-16.
21. Ackermann, S., Menna, F., Scamardella, A., & Troisi, S. (2008, July). Digital photogrammetry for high

- precision 3D measurements in shipbuilding field. In *6th CIRP International Conference on ICME-Intelligent Computation in Manufacturing Engineering*.
22. Tasseti, N., Martelli, M., & Buglioni, G. (2015, June). Reverse engineering techniques for trawler hull 3D modelling and energy efficiency evaluation. In *Proc of NAV 2015 18th International Conference on Ships and Shipping Research* (pp. 24-26).
 23. Burdziakowski, P., & Tysiac, P. (2019). Combined close range photogrammetry and terrestrial laser scanning for ship hull modelling. *Geosciences*, 9(5), 242. <https://doi.org/10.3390/geosciences9050242>
 24. Abbas, M. A., Lichti, D. D., Chong, A. K., Setan, H., Majid, Z., Lau, C. L., ... & Ariff, M. F. M. (2017). Improvements to the accuracy of prototype ship measurement method using terrestrial laser scanner. *Measurement*, 100, 301-310. <https://doi.org/10.1016/j.measurement.2016.12.053>
 25. Menna, F., & Nocerino, E. (2014). Hybrid survey method for 3D digital recording and documentation of maritime heritage. *Applied Geomatics*, 6(2), 81-93. <https://doi.org/10.1007/s12518-011-0074-9>
 26. Martelli, M., Vernengo, G., Bruzzone, D., & Notti, E. (2016, June). Overall efficiency assessment of a trawler propulsion system based on hydrodynamic performance computations. In *The 26th International Ocean and Polar Engineering Conference*. OnePetro.
 27. Çelik, M. Ö., Yakar, İ., Hamal, S., Oğuz, G. M., & Kanun, E. (2020). SfM tekniği ile oluşturulan 3B modellerin kültürel mirasın belgelenmesi çalışmalarında kullanılması: Gözne Kalesi örneği. *Türkiye İnsansız Hava Araçları Dergisi*, 2(1), 22-27.
 28. Yakar, M., & Yılmaz, H. M. (2008). Kültürel miraslardan tarihi Horozluhan'ın fotogrametrik röleve çalışması ve 3 boyutlu modellenmesi. *Selçuk Üniversitesi Mühendislik, Bilim ve Teknoloji Dergisi*, 23(2), 25-33.
 29. Alptekin, A., Çelik, M. Ö., & Yakar, M. (2019). Anıtmezarın yersel lazer tarayıcı kullanarak 3B modellenmesi. *Türkiye Lidar Dergisi*, 1(1), 1-4.
 30. Jing, X., Zhang, C., Sun, Z., Zhao, G., & Wang, Y. (2015, April). The technologies of close-range photogrammetry and application in manufacture. In *3rd International Conference on Mechatronics, Robotics and Automation* (pp. 988-994). Atlantis Press.
 31. Huang, G. P. (2005). Study on the key technologies of digital close range industrial photogrammetry and applications. *Tianjin: Tianjin University*.
 32. Ingeniería y la mecánica (2019). Disc brakes: construction, working principle, types, and rotor materials.
 33. Şahin, İ., Şahin, T., & Gökçe, H. (2017). Hasarlı Dişlilerin Tersine Mühendislik Yaklaşımıyla Yeniden Oluşturulması. *Düzce Üniversitesi Bilim ve Teknoloji Dergisi*, 5(2), 485-495.
 34. Saiga, K., Ullah, A. S., & Kubo, A. (2021). A Sustainable Reverse Engineering Process. *Procedia CIRP*, 98, 517-522. <https://doi.org/10.1016/j.procir.2021.01.144>.
 35. Li, L., Li, C., Tang, Y., & Du, Y. (2017). An integrated approach of reverse engineering aided remanufacturing process for worn components. *Robotics and Computer-Integrated Manufacturing*, 48, 39-50.
 36. Ingle, K. A. (1994). *Reverse engineering*. McGraw-Hill Professional Publishing.



© Author(s) 2022. This work is distributed under <https://creativecommons.org/licenses/by-sa/4.0/>